Reversible lithium insertion and conversion process of amorphous VS_4 revealed by *operando* electrochemical NMR spectroscopy

Keiji Shimoda[a,*], Tomonari Takeuchi[b], Miwa Murakami[a], Hikari Sakaebe[b]

[a] *Office of Society-Academia Collaboration for Innovation, Kyoto University, Uji, Kyoto 611-0011, Japan*

[b] *Research Institute of Electrochemical Energy, National Institute of Advanced Industrial Science and Technology* (*AIST*), *Ikeda, Osaka 563-8577, Japan*

Abstract

Due to the high theoretical capacity, VS_4 is a promising electrode material for next-generation rechargeable batteries. In this study, the lithium insertion and conversion process of amorphous VS_4 was investigated using *operando* electrochemical nuclear magnetic resonance (NMR) spectroscopy. Amorphous VS_4 has a chain-like structure similar to that of crystalline VS_4. The chain structure was drastically changed to the $[VS_4]^{3-}$ tetrahedral structure by lithium insertion up to the Li_3VS_4 composition. The lithium insertion into the $[VS_4]^{3-}$-based structure proceeded further up to the Li_6VS_4 composition, with charge compensation by the reduction of the V valency. Finally, the conversion reaction from amorphous Li_6VS_4 to metallic V and $4Li_2S$ was observed. The structural reversibility of amorphous VS_4 was confirmed after the delithiation. It is worth mentioning that the delithiation process from the conversion products was different from the lithiation, resulting in a relatively large voltage hysteresis. Broadly, this study demonstrates

that the *operando* electrochemical NMR technique is a useful tool for investigating the complex reaction system of non-crystalline battery materials.

Keywords:

Lithium-sulfur battery

Vanadium sulfides

Amorphous transition metal polysulfides

Operando NMR spectroscopy

*Corresponding author:

Keiji Shimoda

Office of Society-Academia Collaboration for Innovation, Kyoto University, Gokasho, Uji 611-0011, Japan

E-mail address: shimoda.keiji.6v@kyoto-u.ac.jp

Tel: +81-774-38-4967

Fax: +81-774-38-4996

1. Introduction

Transition metal (TM) polysulfides, such as TiS_2, VS_2, FeS_2, MoS_2, and VS_4, are one of the promising electrode materials for next-generation rechargeable batteries, due to their high theoretical capacities. Among the commonly available TM polysulfides, VS_4 has the highest amount of sulfur, which translates into the highest theoretical capacity of 1,196 mAh g^{-1}, and therefore, it is considered to be the most promising positive electrode material when Li metal is used as the negative electrode material. VS_4 has a unique crystalline form (patronite), in which an infinite chain along the *c* axis is stabilized by the Peierls distortion with alternate V-V distances of 2.83 and 3.22 Å, and each V^{4+} ion is coordinated by disulfide anions $[S_2]^{2-}$ [1].

The electrochemical performance of crystalline VS_4 (c-VS_4) has been intensively examined. The initial charging capacity of the c-VS_4 electrode composite with reduced graphene oxide (VS_4/rGO) was reported to be 1,105 mAh g^{-1} at a current rate of 0.1 C, and excellent capacity retention of 954 mAh g^{-1} was obtained after 100 cycles [2]. The electrochemical reaction was proposed as $VS_4 + 8Li^+ + 8e^- \rightarrow V + 4Li_2S$ during the initial discharging and $Li_2S \leftrightarrow S + 2Li^+ + 2e^-$ after the subsequent charging process, leaving the metallic V inert [3]. The discharge-charge mechanism of c-VS_4 was investigated using X-ray diffraction (XRD), pair distribution function (PDF) analysis, X-ray absorption spectroscopy (XAS), and solid-state nuclear magnetic resonance (NMR) spectroscopy [4]. The chain structure of c-VS_4 transformed into intermediate lithium insertion phases such as amorphous Li_3VS_4 (a-Li_3VS_4) with $[VS_4]^{3-}$ tetrahedral units, and then to the final conversion products of face-centered cubic (fcc) V and $4Li_2S$ at 0 V. The amorphous/disordered VS_4 phase was partially reformed in the cycled electrode, in contrast with the previous speculation mentioned above [3]. Zhang et al. also suggested that the conversion reaction from c-VS_4 to metallic V and $4Li_2S$ was partially reversible in the first cycle whereas in

the subsequent cycles, an anomalous intercalation/conversion mixed reaction to Li_yVS_4 ($0 < y < 8$) was dominant, owing to the amorphization of c-VS_4 during the first cycle [5]. More recently, Lian et al. proposed stepwise phase changes during lithium insertion after Li_3VS_4 composition, where the separation of Li_2S at each step was suggested based on density functional theory (DFT) calculations [6]. These studies indicate that the lithium insertion and conversion process of c-VS_4 and its reversibility are not yet fully understood.

Recently, amorphous VS_4 (a-VS_4) was synthesized by mechanical milling of c-VS_4 [7]. The discharge-charge profile of a-VS_4 resembles that of c-VS_4, and its cycle performance was improved within the applied voltage window of 1.0–3.0 V [8]. The structural changes of a-VS_4 during the lithiation/delithiation process were investigated using solid-state NMR spectroscopy [9]. The pristine a-VS_4 showed a Peierls-distorted one-dimensional chain structure similar to that of c-VS_4. The chain structure changed immediately during the lithiation to form a-Li_3VS_4, having the $[VS_4]^{3-}$ tetrahedral structure with interstitial Li ions. The Li ions were further incorporated into a-Li_3VS_4, while no conversion to elemental V was observed at 1.5 V. After the first cycle, a highly disordered chain-like structure was recovered. Therefore, reversible lithium insertion/extraction was confirmed in between a-VS_4 and a-Li_xVS_4 ($x \approx 5$) with a high capacity of ~700 mAh g^{-1} using a narrow potential window of 1.5–2.6 V [9]. Based on the structural similarity between c-VS_4 and a-VS_4, a much larger capacity may be delivered by applying a lower potential to ~0 V. However, the full description of lithium insertion and conversion process of a-VS_4, which would occur below 1.5 V, has not been verified. The structural reversibility of a-VS_4 is also unclear when the cell is discharged to ~0 V. A detailed understanding of the lithiation/delithiation process of a-VS_4 is also essential for that of c-VS_4 since c-VS_4 changes to be amorphous after the initial discharging [4].

Solid-state NMR spectroscopy is a beneficial technique for investigating the chemical environments on a specific element both in crystalline and non-crystalline materials. *Operando* and/or *in-situ* NMR technique can quantitatively characterize spectral (structural) changes in a single experiment in a non-destructive manner, despite its poorer spectral resolution compared to the *ex-situ* magic-angle spinning (MAS) technique. The *operando* ^{7}Li NMR measurements were found to be very useful for investigating the structural changes in a-VS_4 during lithiation [9]. In this brief report, we discuss the comprehensive structural changes of a-VS_4 during the lithium insertion and conversion process and its structural reversibility using the *operando* electrochemical NMR technique.

2. Experimental

The experimental procedures have been described elsewhere [9]. Briefly, crystalline VS_4 was synthesized using V_2S_3 (99%, Kojundo Chemical Laboratory) and S (99.9%, Wako). The mixture was sealed in a glass tube under vacuum and heated twice at 400 °C for 12 h [10]. Then, amorphous VS_4 was prepared from crystalline VS_4 by mechanical milling for 40 h at 270 rpm in a planetary ball mill (Pulverisette 7, Fritsch). The working electrode consisted of a mixture of the active material (a-VS_4), Ketjen Black (KB), and polytetrafluoroethylene (PTFE) binder in a weight ratio of 59:29:12 on a Ni mesh current collector. A Li foil (0.2 mm in thickness, >99.9%, Honjo Metal) was used as the negative electrode, and a microporous polyolefin sheet was chosen as separator. A solution of 1 M $LiPF_6$ dissolved in a 3:7 volume ratio mixture of ethylene carbonate (EC) and ethyl methyl carbonate (EMC) was used as the electrolyte solution (Kishida Chemical). Inductively coupled plasma-atomic emission spectrometry (ICP-AES) measurements indicated that the dissolution of polysulfide species was negligible in the carbonate-based electrolyte solutions. Two-electrode laminate cells were assembled in an Ar-filled glove box. The

electrochemical measurements were performed at 30 °C (HJ1001SD8, Hokuto Denko). The cells were galvanostatically cycled twice between 0.2 and 3.0 V at a current density of 59.8 mA g^{-1} (0.05 C rate, 1 C = 1,196 mA g^{-1}) during the NMR measurements (total measurement time of 74 h). A cell was then carefully disassembled at 0.2 V in the glove box and rinsed with dimethyl carbonate (DMC) to remove the residual electrolyte solution for *ex-situ* NMR measurements.

NMR spectra were acquired on a DD2 600 spectrometer (Agilent Technologies) at a magnetic field of 14.1 T. *Operando* ^{7}Li NMR measurements were performed with a homemade wide-bore static probe, in which a flat laminate cell was placed parallel to the magnetic field (vertical setting) in the center of a 10 mm-diameter solenoid coil. The laminate cell and probe head are shown in Fig. S1. A Hahn echo pulse sequence was used with a first pulse width of 4.5 μs, an echo decay of 8 μs, and a relaxation delay of 1 s. Each spectrum was averaged over 10 min during the electrochemical cycling (443 spectra for 74 h). After the *operando* electrochemical NMR measurements, ^{7}Li and ^{51}V MAS NMR spectra were acquired for samples disassembled from the laminate cells, with a wide-bore T3 MAS probe (Agilent Technologies). The powdered samples were packed into 1.2 mmϕ MAS ZrO_2 rotors with airtight caps in an Ar-filled glove box and spun at a rate of 60 kHz during the measurements. A rotor-synchronized Hahn echo pulse sequence (π/2-τ-π-τ-acq.) was used with a π/2 pulse width of 1.0 μs and a relaxation delay of 5 s for ^{7}Li MAS measurements, along with 0.5 μs and 0.5 s for ^{51}V MAS measurements, respectively. All spectra were referenced to 1 M LiCl solution (0.0 ppm) and V_2O_5 (–612 ppm) for ^{7}Li and ^{51}V nuclei, respectively.

3. Results and discussion

Fig. 1 shows the XRD profile of a-VS_4 along with that of c-VS_4. The diffraction peaks were lost, and a broad halo pattern was observed at ~15° for a-VS_4. The detailed structural characterization of pristine a-VS_4 is provided elsewhere [9].

To understand the lithiation/delithiation behavior of a-VS_4, *operando* ^{7}Li NMR measurements were performed. Fig. 2 shows the *operando* ^{7}Li NMR spectra of the a-VS_4 electrode, which was cycled twice at a current rate of 0.1 C in a voltage window of 1.5–2.6 V. The delivered discharging/charging capacities in the first and second cycles were 720/670 and 668/661 mAh g^{-1}, respectively (Fig. S2a). The discharging capacity of 720 mAh g^{-1} corresponds to a composition close to that of Li_5VS_4, assuming that contributions from electrolyte decomposition are small. Here, the difference spectra subtracting the initial spectrum before the electrochemical test are provided in Fig. 2 to cancel out a large signal from the $LiPF_6$ salt in the electrolyte solution at ~0 ppm. A broad signal was appeared at ~26 ppm and increased in intensity during the early lithiation process. This signal is ascribed to Li ions in amorphous Li_3VS_4 (a-Li_3VS_4) [9]. Previous studies have suggested that a-Li_3VS_4 has $[VS_4]^{3-}$ tetrahedral units [4,9]. This indicates that S-S disulfide bonds and chain structure of a-VS_4 were broken, and the $[VS_4]^{3-}$ tetrahedral structure of a-Li_3VS_4 was formed by lithium insertion. The $[VS_4]^{3-}$ tetrahedron has diamagnetic V^{5+} ($3d^0$ electronic configuration) and S^{2-} ions, indicating the oxidation of V ions as well as the reduction of S ions. The *operando* spectra indicated that lithium insertion proceeded in a two-phase reaction between a-VS_4 and a-Li_3VS_4. The spectral evolution was altered with an increase in the Li content above Li_3VS_4. The signal shifted to higher frequencies with a significant increase in the linewidth and a decrease in the integrated intensity (Fig. 2). These behaviors suggest increasing Fermi contact and dipolar interactions between the ^{7}Li nuclei and the unpaired electrons on the V ions [11]. The intensity loss may be attributed to the incomplete RF excitation/detection of the broader signal component. Therefore, charge compensation is

achieved by the reduction of V valence, and the paramagnetic V^{4+} ($3d^1$) and V^{3+} ($3d^2$) ions become dominant in a-$Li_{3+d}VS_4$ ($0 < d \leq 2$). Finally, a-Li_5VS_4 was obtained at 1.5 V. On the subsequent delithiation, the signal position of a-$Li_{3+d}VS_4$ shifted back to lower frequencies, and its linewidth decreased subsequently. The peak position of the recovered a-Li_3VS_4 was located at ~11 ppm, with a relatively narrow linewidth. This suggests that the structure of a-Li_3VS_4 formed during delithiation is different from that of lithiation product. The ^{7}Li signal of a-Li_3VS_4 completely disappeared at the end of the charge, where the recovery of the disordered chain structure of a-VS_4 was demonstrated [9]. The spectral evolution observed in the second cycle was identical as found in the first cycle, indicating that the structural changes are fully reversible.

Fig. 3 shows the *operando* ^{7}Li NMR spectra (difference spectra) of the a-VS_4 electrode cycled twice at a current rate of 0.05 C in a voltage window of 0.2–3.0 V. The representative spectra of the Li_xVS_4 composition (x = 0–8) are shown in Fig. S3. The delivered discharging/charging capacities in the first and second cycles were 1,195/1,017 and 1,025/974 mAh g^{-1}, respectively (Fig. S2b). The initial discharge capacity coincides with the theoretical capacity (1,196 mAh g^{-1}; $VS_4 + 8Li^+ + 8e^- \leftrightarrow V + 4Li_2S$). A broad signal of a-$Li_3VS_4$ first appeared, and then, the signal of a-$Li_{3+d}VS_4$ shifted to higher frequencies with a significant increase in linewidth, as shown in Fig. 2. The highest frequency was obtained for a-Li_5VS_4. Subsequently, the signal shifted back to lower frequencies, with the decrease in its width, and the integrated intensity again increased as voltage decreased below 1.5 V. These behaviors suggest decreasing Fermi contact and dipolar interactions between the ^{7}Li nuclei and the unpaired electrons on the V ions. This corresponds to the formation of a-$Li_{3+d}VS_4$ ($2 < d < 4$). Here, the electronic configuration of the V^{2+} ($3d^3$) ion in a-Li_6VS_4 is interpreted as in a low-spin state $e^3t_2^0$ in the $[VS_4]^{3-}$ tetrahedron. Therefore, it is reasonable to consider that the $[VS_4]^{3-}$ tetrahedral units are preserved in a-$Li_{3+d}VS_4$ ($0 < d < 4$)

when Li ions are further inserted into a-Li_3VS_4. If the V^+ ion in the $3d^4$ configuration is diamagnetic (i.e., a low-spin state $e^4t_2^0$ for T_d symmetry), the peak position of a-Li_7VS_4 would be close to that of a-Li_3VS_4. However, the actual peak position and linewidth at the Li_7VS_4 composition were similar to those of the Li_8VS_4 composition (Fig. S3a), where the conversion products of metallic V and $4Li_2S$ were formed. The broad signal centered at ~5 ppm in the Li_7VS_4 and Li_8VS_4 compositions is assigned to Li_2S. Therefore, the conversion products are formed through the decomposition of a-Li_6VS_4 by further lithium insertion. The ^{7}Li and ^{51}V MAS NMR spectra for the sample disassembled at 0.2 V confirmed the formation of Li_2S and metallic V (Fig. S4). The ^{51}V Knight-shift signal at ~5650 ppm was ascribed to fcc V, and the a-VS_4 and a-Li_3VS_4 signals were completely disappeared [4,9]. Additionally, electrolyte decomposition was found to be accelerated when the voltage decreased below 1.5 V, which is manifested as a relatively sharp peak at ~0 ppm in the *operando* ^{7}Li spectra (Figs. 3 and S3).

Lian et al. investigated the possible structural transition pathway during lithiation of c-VS_4 by calculating the formation enthalpies of tentative crystalline/amorphous Li_xVS_4 and possible decomposition phases [6]. They proposed stepwise phase separation during lithium insertion after Li_3VS_4 composition, where Li_2S was separated at each step. For the Li_4VS_4 composition, the calculation showed that the decomposition products of $VS_2 + 2Li_2S$ were energetically most stable, although they concluded that c-Li_4VS_4 was the expected material, considering the large energy barrier for the reaction path (c-$Li_4VS_4 \rightarrow$ a-$Li_4VS_4 \rightarrow VS_2 + 2Li_2S$). Similarly, the decomposition products of $Li_3VS_3 + Li_2S$ and $VS + 3Li_2S$ were proposed for the Li_5VS_4 and Li_6VS_4 compositions, respectively. Our results differ from these expected reactions and decomposition products because the decomposition product of Li_2S was not observed in the *operando* NMR spectra up to the Li_7VS_4 composition (Fig. S3a). The discrepancy between the

experiment and calculation could be attributed to the large energy barrier for the structural relaxation, including long-range atomic diffusion, from the energetically metastable a-$Li_{3+d}VS_4$ to the stable decomposition products.

The spectral evolution during delithiation was distinctly different from that during lithiation (Figs. 3 and S3). During delithiation, the signal of Li_2S first decreased in intensity. The signal was broader in linewidth at the Li_6VS_4 and Li_5VS_4 compositions (Fig. S3b). However, clear evidence of paramagnetic V ions in proximity to Li ions was not provided because of the lack of large peak shifts. This may suggest the formation of vanadium sulfides, VS + $3Li_2S$ and VS_2 + $2Li_2S$ at the Li_6VS_4 and Li_4VS_4 compositions, respectively, which were proposed in the DFT work [6]. It is reasonable to consider that VS + $3Li_2S$ and VS_2 + $2Li_2S$, or more generally, VS_y + $(4–y)Li_2S$, are more plausible than the formation of a-$Li_{3+d}VS_4$ when Li ions are extracted from the conversion products of V + $4Li_2S$. Li_2S changes to elemental S, and the S atom then reacts with metallic V. The peak position of the signal at the Li_4VS_4 and Li_3VS_4 compositions was close to that of the recovered a-Li_3VS_4 (Fig. 2), although the former signal was much broader in linewidth. Therefore, a highly disordered a-Li_3VS_4 would be recovered. At the end of charging, the signal of a-Li_3VS_4 completely disappeared, leaving only the signal caused by electrolyte decomposition. The recovered a-Li_3VS_4 changed back to a-VS_4 in the two-phase reaction, which is shown as a voltage plateau. The chain-like structure was recovered in the cycled a-VS_4, and the spectral evolution in the second cycle was almost the same as that in the first cycle. Therefore, the structural changes are repeated in the second cycle, in contrast to the previous studies [3,5]. The signal of a-Li_xVS_4 appeared to be broadened in the second cycle, suggesting increasing structural disordering. The proposed lithiation/delithiation pathway is summarized in Fig. 4. This study is useful to re-evaluate the lithiation/delithiation process and structural reversibility of c-VS_4.

4. Conclusions

We investigated the lithium insertion (from a-VS_4 to a-$Li_{3+d}VS_4$) and conversion process (from a-$Li_{3+d}VS_4$ to V + 4Li_2S) of mechanically prepared a-VS_4 using *operando* electrochemical ^{7}Li NMR spectroscopy. The local structure of the as-prepared a-VS_4 consisted of a one-dimensional chain structure showing the Peierls distortion. By lithium insertion into a-VS_4, amorphous Li_3VS_4 (a-Li_3VS_4) was first formed through a two-phase reaction, where the $[VS_4]^{3-}$ tetrahedral units were built by breaking the chain structure. Further lithium insertion into a-Li_3VS_4 was associated with the reduction of V ions, which is shown by the positive peak shifts and line broadening in the *operando* ^{7}Li NMR spectra. At around Li_7VS_4 composition, the tetrahedral structure in a-$Li_{3+d}VS_4$ (d < 4) became unstable and decomposed to the final conversion products of metallic V and 4Li_2S. The delithiation process from the conversion products was different from the lithiation. The Li ions were extracted from Li_2S, and vanadium sulfides (VS_y) would be formed, instead of a-$Li_{3+d}VS_4$ (d < 4), during the early half of the delithiation process. This causes a relatively large voltage hysteresis. Furthermore, a-Li_3VS_4 was reformed, and the chain-structured a-VS_4 was recovered. Such a reversible lithium insertion and conversion process is feasible between a-VS_4 and V + 4Li_2S with a high capacity of ~1,000 mAh g^{-1} when a wide voltage window is applied. It should be emphasized that this work demonstrates the usefulness of the *operando* electrochemical NMR technique for investigating the complex reaction path of non-crystalline battery materials.

Acknowledgments

This work was supported by the Research and Development Initiative for Scientific Innovation of New Generation Batteries 2 (RISING2) funded by the New Energy and Industrial Technology

Development Organization (NEDO), Japan (JPNP16001). The authors thank Mr. Takashi Moroishi for his support with the NMR measurements.

Appendix A. Supplementary data

Supplementary data related to this article can be found online at ****.

References

[1] R. Allman, I. Baumann, A. Kutoglu, H. Rosch, E. Hellner, Sci. Nat., 51 (1964) 263-264.

[2] C.S. Rout, B.H. Kim, X. Xu, J. Yang, H.Y. Jeong, D. Odkhuu, N. Park, J. Cho, H.S. Shin, J. Am. Chem. Soc., 135 (2013) 8720-8725.

[3] X. Xu, S. Jeong, C.S. Rout, P. Oh, M. Ko, H. Kim, M.G. Kim, R. Cao, H.S. Shin, J. Cho, J. Mater. Chem. A, 2 (2014) 10847-10853.

[4] S. Britto, M. Leskes, X. Hua, C.A. Hebert, H.S. Shin, S. Clarke, O. Borkiewicz, K.W. Chapman, R. Seshadri, J. Cho, C.P. Grey, J. Am. Chem. Soc., 137 (2015) 8499-8508.

[5] L. Zhang, Q. Wei, D. Sun, N. Li, H. Ju, J. Feng, J. Zhu, L. Mai, E.J. Cairns, J. Guo, Nano Energy, 51 (2018) 391-399.

[6] R. Lian, J. Feng, D. Wang, Q. Yang, D. Kan, M. Mamoor, G. Chen, Y. Wei, ACS Appl. Mater. Interfaces, 11 (2019) 22307-22313.

[7] K. Koganei, A. Sakuda, T. Takeuchi, H. Sakaebe, H. Kobayashi, H. Kiuchi, T. Fukunaga, E. Matsubara, 69th Annual Meeting of the International Socirty of Electrochemistry, (2018) S06-028 (abstract).

[8] K. Koganei, A. Sakuda, T. Takeuchi, H. Kiuchi, H. Sakaebe, Electrochemistry, 89 (2021) 239-243.

[9] K. Shimoda, K. Koganei, T. Takeuchi, T. Matsunaga, M. Murakami, H. Sakaebe, H. Kobayashi, E. Matsubara, RSC Adv., 9 (2019) 23979-23985.

[10] K. Koganei, A. Sakuda, T. Takeuchi, H. Sakaebe, H. Kobayashi, H. Kageyama, T. Kawaguchi, H. Kiuchi, K. Nakanishi, M. Yoshimura, T. Ohta, T. Fukunaga, E. Matsubara, Solid State Ion., 323 (2018) 32-36.

[11] C.P. Grey, N. Dupre, Chem. Rev., 104 (2004) 4493-4512.

[12] K. Momma, F. Izumi, J. Appl. Crystallogr., 44 (2011) 1272-1276.

Figures and Figure captions

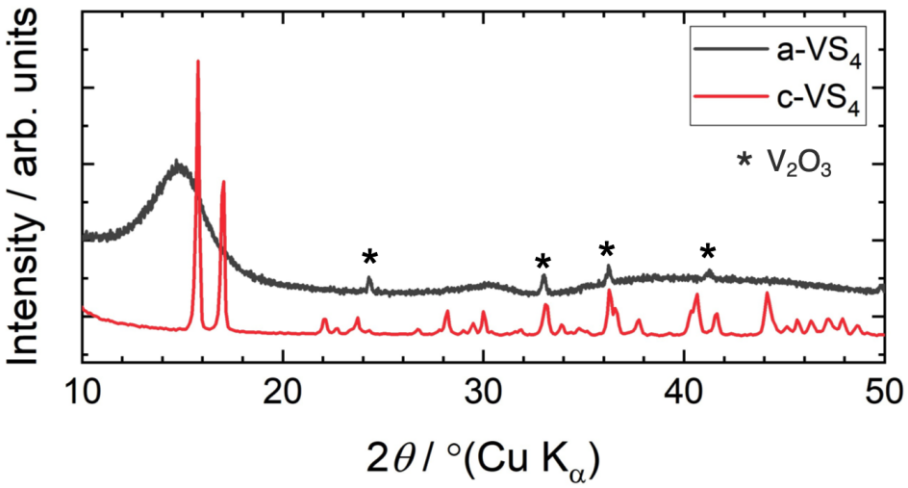

Fig. 1. X-ray diffraction profiles of amorphous VS_4 (a-VS_4) and crystalline VS_4 (c-VS_4).

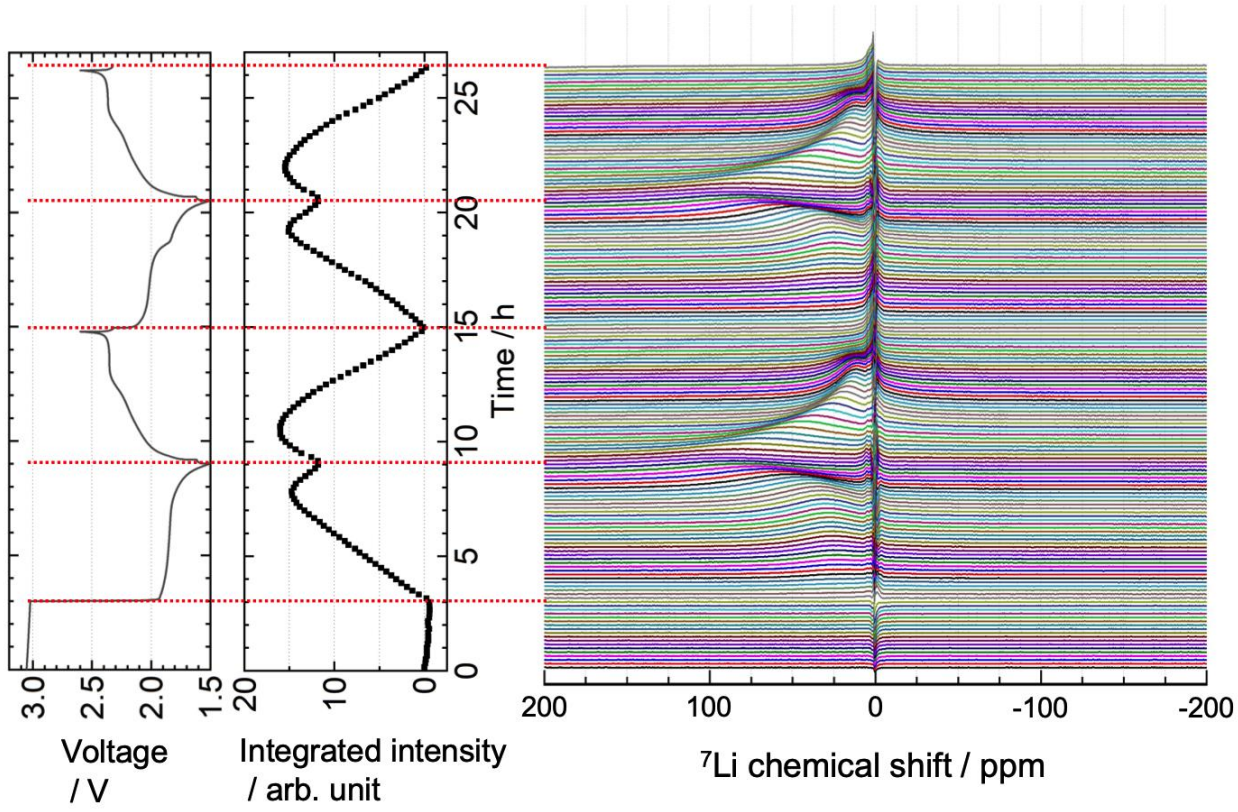

Fig. 2. Time evolution of *operando* ^{7}Li NMR spectra of the Li//a-VS_4 cell, along with the discharge-charge profile and integrated intensity plot of the a-Li_xVS_4 signal. The cell was cycled at a current rate of 0.1 C in the voltage window of 1.5–2.6 V. The red dotted lines indicate the start of the discharge or charge process.

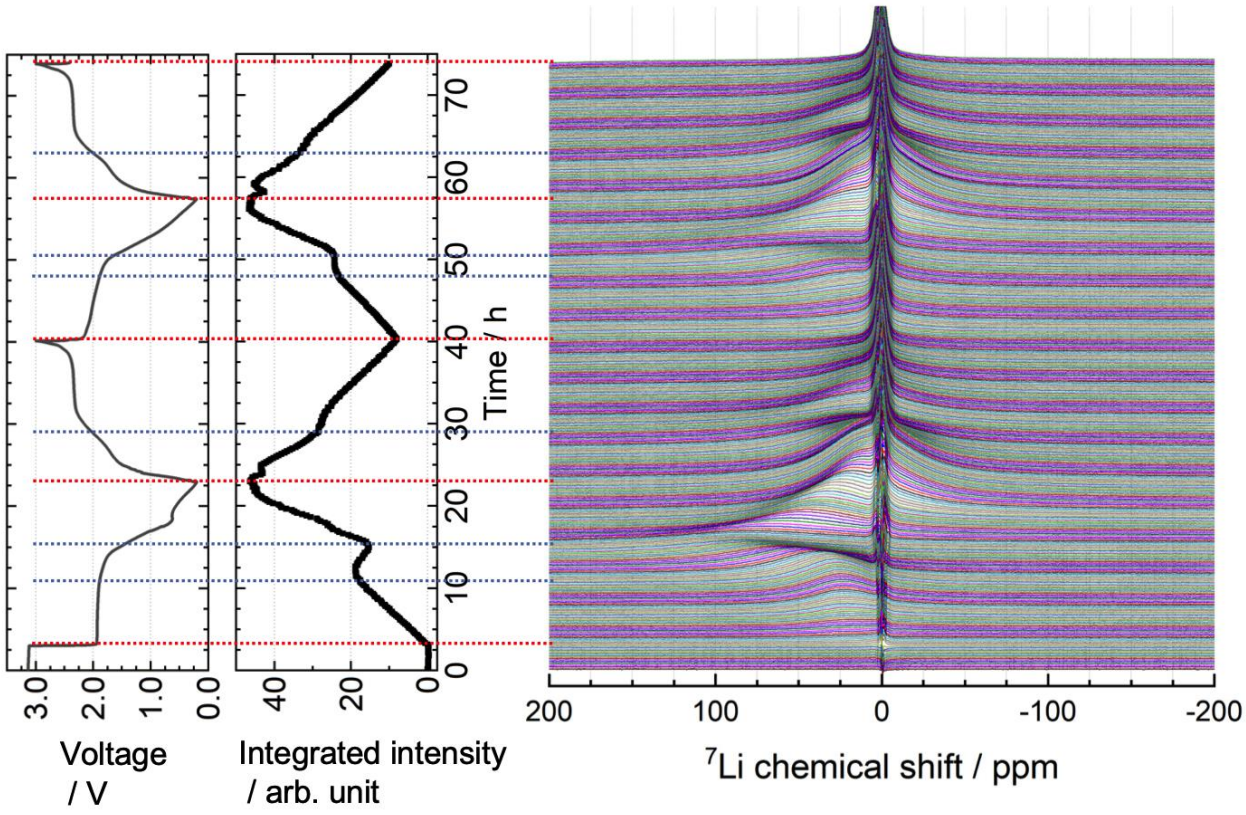

Fig. 3. Time evolution of *operando* ^{7}Li NMR spectra of the Li//a-VS_4 cell, along with the discharge-charge profile and integrated intensity plot of the a-Li_xVS_4 signal. The cell was cycled at a current rate of 0.05 C in the voltage window of 0.2–3.0 V. The red dotted lines indicate the start of the discharge or charge process. The blue dotted lines correspond to some inflection points in the NMR intensity variation.

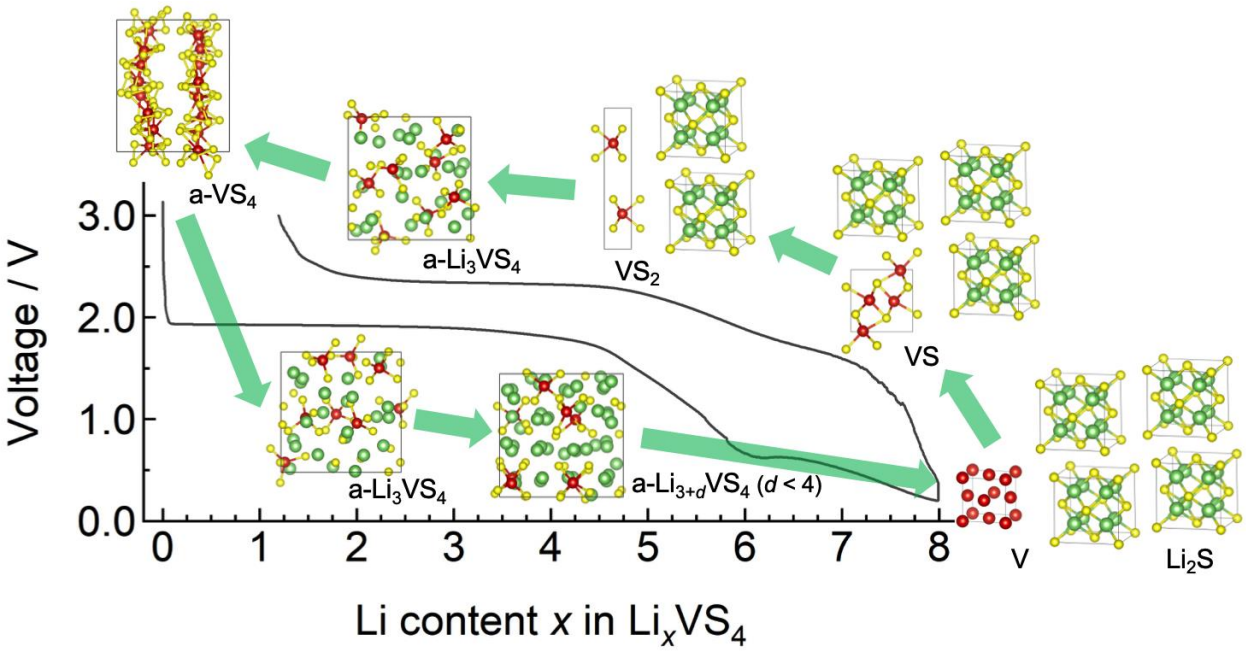

Fig. 4. Schematic illustration of the lithiation/delithiation pathway proposed for a-VS_4. The tentative structure of VS (mp-1868) was obtained from the Materials Project database. The model structures were drawn with VESTA [12]. Green, red, and yellow balls represent Li, V, and S atoms, respectively.